Formation of Stripelike Flux Patterns Obtained by Freezing Kinematic Vortices in a Superconducting Pb Film

A. V. Silhanek,[1] M. V. Milošević,[2] R. B. G. Kramer,[1] G. R. Berdiyorov,[2] J. Van de Vondel,[1] R. F. Luccas,[3] T. Puig,[3] F. M. Peeters,[3] and V. V. Moshchalkov[1]

[1]*INPAC-Institute for Nanoscale Physics and Chemistry, Nanoscale Superconductivity and Magnetism Pulsed Fields Group, Katholieke Universiteit Leuven, Celestijnenlaan 200 D, B-3001 Leuven, Belgium*

[2]*Departement Fysica, Universiteit Antwerpen, Groenenborgerlaan 171, B-2020 Antwerpen, Belgium*

[3]*Institut de Ciencia de Materials de Barcelona, CSIC, Campus de la UAB, 08193 Bellaterra, Spain*

(Received 13 July 2009; published 7 January 2010)

We demonstrate experimentally and theoretically that the dissipative state of superconducting samples with a periodic array of holes at high current densities consists of flux rivers resulting from a short-range attractive interaction between vortices. This dynamically induced vortex-vortex attraction results from the migration of quasiparticles out of the vortex core (kinematic vortices). We have directly visualized the formation of vortex chains by scanning Hall probe microscopy after freezing the dynamic state by a field cooling procedure at a constant bias current. Similar experiments carried out in a sample without holes show no hint of flux river formation. We shed light on this nonequilibrium phenomena modeled by time-dependent Ginzburg-Landau simulations.

DOI: 10.1103/PhysRevLett.104.017001 PACS numbers: 74.78.−w, 05.65.+b, 74.25.F−, 74.25.Uv

Self-organization and its associated pattern morphologies belong to the most striking phenomena in nature. Usually periodic, such features are often the result of competing interactions. One of the most common structures is stripe patterns, which are found in magnetic, colloidal, or biological systems [1]. In most of them, the long-range (dipolarlike) repulsion is balanced by a short-range attraction, with an origin specific to each system.

An interesting analogue can be found in superconductivity. Although this state of matter is magnetophobic, the magnetic field can penetrate (type-II) superconductors in the form of vortices with each bearing a flux quantum Φ_0. Since the magnetic energy increases when vortices approach each other [2], their interaction is purely repulsive, and they form a triangular lattice. However, an attractive component in the vortex-vortex interaction may appear even in type-II superconductors. For example, such phenomenon is observed in anisotropic superconductors with a magnetic field tilted away from the principal symmetry axes [3–5], or as a result of the nonlocal relationship between supercurrents and vector potential in clean and low-κ materials [6]. Another example can be found in the case of type-1.5 superconductors where two weakly coupled order parameters, each of which belong to a different type of superconductivity, coexist in the same material [7,8]. In all cases when vortex attraction is present, a vortex chain formation is observed.

However, the formation of vortex chains in isotropic type-II superconductors is still energetically unfavorable due to purely repulsive interactions [9]. The only instance where vortex chains are predicted to attract each other in type-II isotropic superconductors is when they are *out of equilibrium*. Namely, in an applied dc drive, fast moving vortices due to a Lorentz force create an excess of quasiparticles behind themselves generating a wake of depleted order parameter [10,11]. This effect gives rise to the so-called kinematic vortices characterized by a very anisotropic vortex core elongated in the direction of motion [11]. Under these circumstances, vortices attract the following vortices and interconnect into a ''vortex river.'' This directional interaction between kinematic vortices is indeed similar to several soft-matter systems [12,13], with a difference that vortex rivers are *dynamic*.

In this Letter we image dynamically induced vortex chains by promoting the proliferation of kinematic vortices in the sample via (i) a dc electric current and (ii) by structuring the film with a periodic array of antidots. The reason for patterning is twofold. First, the narrow constrictions between the antidots favor the appearance of kinematic vortices [14] and also magnify the current density. Second, the multiply connected structure permits the stabilization of stationary vortex chains. In what follows, we show direct visualization of vortex stripes by scanning Hall probe microscopy (SHPM) after *"freezing" the dynamic phase* by quickly cooling the sample in the presence of a bias current and applied field.

The investigated sample was a 50 nm thick Pb film with a square array of square antidots made by e-beam lithography and subsequent lift-off. The sample is deposited on top of a Si/SiO_2 substrate. The period of the pattern is $w = 1.5\ \mu$m and the size of the antidots is $a = 0.6\ \mu$m (see the inset of Fig. 1). The average roughness of the Pb film is 1.2 nm on an area of 1 μm^2. In all cases the external field was applied perpendicular to the plane of the film and therefore to the current direction. Transport measurements performed in a sister sample show clear commensurability effects (i.e., enhancements of the critical current) at $H/H_1 = 1/2,\ 1,\ 3/2$, and 2, where $H_1 = \Phi_0/w^2 = 0.92$ mT.

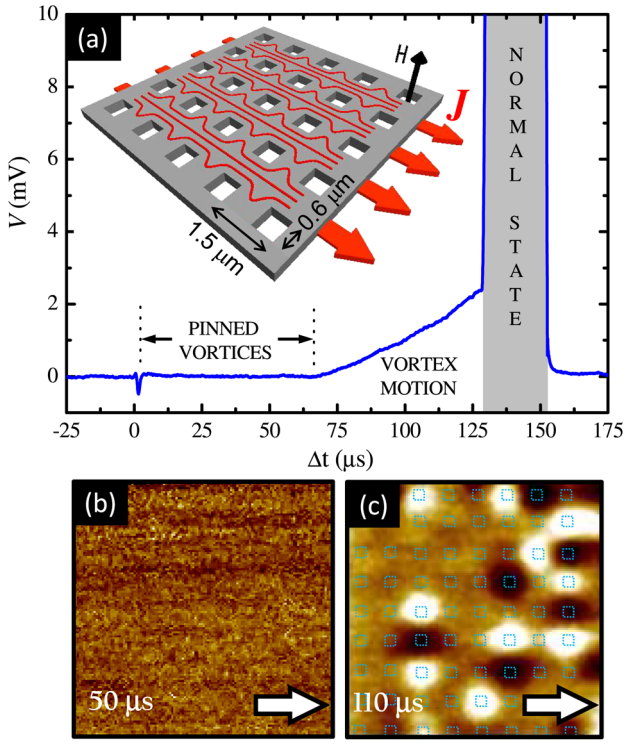

FIG. 1 (color online). (a) Voltage signal as a function of time (Δt) for a 150 μs current pulse of 90 mA amplitude. The inset shows an oblique view of the sketched system consisting of a superconducting film with a periodic array of antidots, in an applied magnetic field H and dc current J. The lines illustrate the inhomogeneous current distribution due to the array of antidots. (b) Differential images obtained by subtracting two consecutive pictures for $\Delta t = 40$ and 50 μs and (c) for $\Delta t = 110$ and 100 μs, for $H/H_1 = 0.1$. The black (white) spots indicate the initial (final) position of vortices before (after) the last pulse. The frames in (b) and (c) are 13.5×13.5 μm^2. The arrows indicate the direction of the applied current.

From the superconducting phase boundary of an unpatterned Pb film we obtain the superconducting coherence length $\xi(0) \sim 33$ nm and critical temperature $T_c = 7.2$ K. All samples were patterned in a 300 μm wide and 2.1 mm long transport bridge with voltage contacts which permitted transport measurements and SHPM to be done simultaneously. The microscopy images were taken with a commercial SHPM [15] after field cooling (FC) the sample. At 4.2 K, the scanning area is $\sim 13 \times 13$ μm^2. The Hall sensor sits about 500 nm above the surface of the sample. Under these conditions vortices in Pb produce a maximum signal of $\sim$2.5 G whereas the field resolution of the Hall cross is better than 0.1 G.

Our experimental results are supported by a theoretical analysis based on the time-dependent Ginzburg-Landau (TDGL) formalism and solving the equation [16]

$$\frac{u}{\sqrt{1+\Gamma^2|\psi|^2}}\left(\frac{\partial}{\partial t} + i\varphi + \frac{\Gamma^2}{2}\frac{\partial|\psi|^2}{\partial t}\right)\psi = (\nabla - i\mathbf{A})^2\psi + (1 - T - |\psi|^2)\psi, \quad (1)$$

coupled with the equation for the electrostatic potential $\Delta\varphi = \mathrm{div}[\mathrm{Im}(\psi^*(\nabla - i\mathbf{A})\psi)]$ in a self-consistent Euler iterative procedure. All quantities in Eq. (1) are scaled to units at zero temperature, distances to coherence length $\xi(0)$, time to $\tau_{\mathrm{GL}} = \pi\hbar/8k_BT_cu$, the electrostatic potential to $\varphi_0 = \hbar/2e\tau_{\mathrm{GL}}$, and vector potential $\mathbf{A}$ to $\Phi_0/2\pi\xi(0)$. In Eq. (1), $\Gamma = 2\tau_E\psi_0/\hbar \sim 10$, with τ_E the inelastic scattering time, ψ_0 the order parameter at $H = 0$, and $u = 5.79$ [16]. Neumann boundary conditions for ψ and φ are applied at all sample boundaries (including antidots), except at the interface with lateral current leads where $\nabla\varphi\,|_n = -j$.

Prior to transport experiments, we took a series of images at 4.2 K after the FC procedure with fields ranging from -4 to $+4$ mT in steps of 0.02 mT. We observed a variety of commensurate vortex states [17–20], and determined that a maximum of two flux quanta can be trapped in each antidot, in agreement with Ref. [17]. Our first attempts to simultaneously record images while moving vortices with an external dc current showed that vortices remain pinned until reaching the critical current beyond which severe heat dissipation drives the sample to the normal state. This transition is very abrupt and we were unable to visualize the actual vortex motion. To overcome this experimental shortcoming we applied current pulses to minimize heating effects.

Figure 1(a) shows a typical voltage response for a pulse of 150 μs duration and amplitude 90 mA obtained at $H/H_1 = 0.1$ and temperature $T = 7$ K. Three clear regimes can be identified: at short times no dissipation is observed, at intermediate times the voltage signal monotonically increases as a function of time indicating a progressive heating of the sample, and for long pulses the system transits abruptly to the normal state. Interestingly, the images obtained after applying pulses of long duration are identical to those obtained by field cooling procedure. Namely, long pulses heat the sample above T_c and, therefore, once the bias current is switched off (nanoseconds) the thermal relaxation of the sample towards the original temperature takes about 100 ms [21]. This (unconventional) field cooling procedure is very convenient and fast since it enables us to heat the sample without warming up the rest of the bulky addenda.

For short enough current pulses the superconducting state was sustained in the sample, and we searched for evidence of vortex motion under Lorentz force. The protocol used for visualizing the vortex dynamics was (1) the sample is cooled down at a given field, (2) a short 50 μs long current pulse is applied, (3) an image scan is performed, and (4) a new pulse, 10 μs longer than the previous pulse, is applied. Then, steps (3) and (4) were repeated until superconductivity was destroyed. In the lower panels of Fig. 1 we show the differential images, obtained by subtracting two consecutive scans, for short [1(b)] and intermediate pulse duration [1(c)]. The lack of any contrast in Fig. 1(b) indicates that short pulses are unable to set vortices in motion. In contrast to that, pulses of intermedi-

ate duration lead to a clear vortex motion, visible in Fig. 1(c) through pairs of black (vortex disappearance) and white spots (vortex appearance) compared to the previous image.

Of course, the vortex mobility is highly dependent not just on the duration of the current pulse but on the amplitude of the pulse as well. Besides this expected behavior, in Fig. 2 we show a nontrivial dependence of vortex mobility on applied magnetic field, both experimentally determined and theoretically simulated. Namely, the number of moved vortices after a pulse depends on the vortex density in comparison to the density of pinning sites. In the vicinity of matching fields $H = nH_1$, the rigidity of the pinned vortex lattice prevents the individual vortex motion. The minima of vortex mobility are found close to integer-matching fields, where vortices form a highly ordered lattice with no available places to hop in [22].

After determining the needed pulse duration for vortex motion, we subjected the sample to a series of pulses of intermediate width with a long delay between two consecutive pulses. Figure 3 shows images of the vortex distribution obtained at $T = 6.5$ K immediately after field cooling at $H \sim H_{1/2}$ [3(a)] and after a series of 100 μs pulses with 36 mA amplitude [3(b)] [corresponding images from theoretical simulations are given in Figs. 3(c) and 3(d)]. Strikingly, after applying the train of pulses, the vortex lattice is neither fully disordered nor similar to the equilibrium FC image, but instead exhibits a clear tendency of vortices towards alignment. Observed vortex rows in Fig. 3(b) follow both principal directions of the underlying pinning potential. This is understood from the known rearrangement of vortex lattice under applied drive [11]. Namely, prior to phase slippage in the aforementioned samples, the simulations show that the vortex lattice in motion rearranges towards a square lattice. This nonequilibrium feature is made stationary in our samples due to the antidot lattice which pins the partially rearranged vortex lattice, as shown in Fig. 3. As shown in Fig. 3(d), after the current pulse, vortices are trapped in parallel rows, as their dynamic preparation for continuous motion across the sample is intercepted.

We hereby realized that the known nonequilibrium states can be *equilibrated* in our sample. To investigate this point further, we employed an alternative method by cooling the sample while maintaining a dc current through it. In this way we avoid the heating issues upon cooling, and freeze the vortex structure at a resultant (current-dependent) temperature T_f. Because of the irreversible behavior of the current-voltage characteristics, differences with respect to the pulsed-current procedure may be expected. Figure 4 shows a selected set of images after field cooling down to $T = 4.2$ K with different magnetic fields without applied current (top row) and with an applied current of 36 mA (bottom row). The most pronounced features of this figure are the parallel (and frozen) *rivers of flux*. This unique state is composed of vortices trapped by antidots, in linear chains which are presumed to be unstable in type-II superconductors. This is the primary result of this Letter, showing the history-dependent metastability of vortex states in the presence of pinning (measurements performed in a coevaporated plain unpatterned Pb film under identical conditions show no hint of stripe formation [23]), and the existence of an attractive interaction between vortices when moving at high velocities.

The number of observed vortex rivers inside the scanning area is two, irrespective of the applied magnetic field. It is important to notice that since the sample is acting as a microheater, the control of cooling rates with an external thermometer is meaningless. The importance of the actual cooling rate ζ_T is highlighted in Fig. 5, where the calculated voltage $V(T)$ is shown for four different cooling rates. We found that fast cooling is of prime importance for the "freezing" of kinematic vortex lines, as only the fastest sweep of temperature resulted in good agreement with experimental observations [see images 5(a)–5(c)]. At slower cooling rates, the vortex state equilibrates at lower temperatures towards latticelike structures (i.e., no vortex rivers).

It is worth mentioning that SHPM images taken at the border of the sample showed that at $T = 6$ K a current of

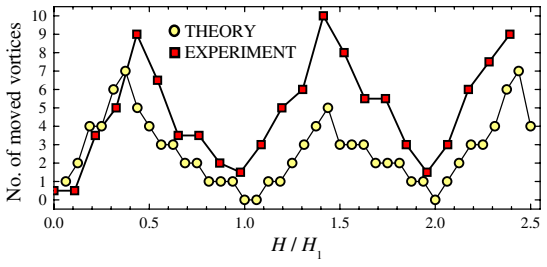

FIG. 2 (color online). Number of displaced vortices as a function of applied field after a current pulse of fixed amplitude and duration—experiment versus theory. The experimental data were obtained at $T = 6.5$ K with pulses of 36 mA amplitude.

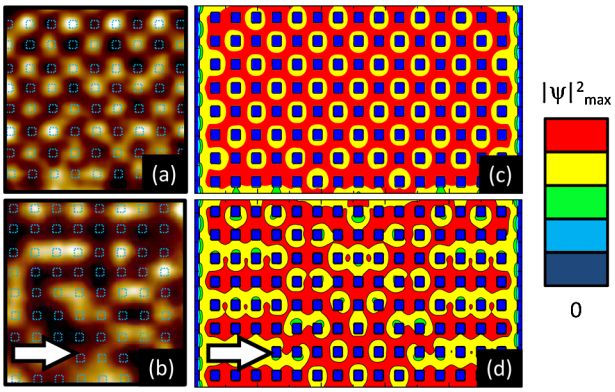

FIG. 3 (color online). SHPM image obtained at $T = 6.5$ K and $H = H_{1/2}$ after field cooling (a) and after current pulses of duration 100 μs and amplitude 36 mA (b). Panels (c) and (d) are the corresponding images from TDGL simulations on a 12×24 μm^2 sample. The arrows indicate the direction of the applied current.

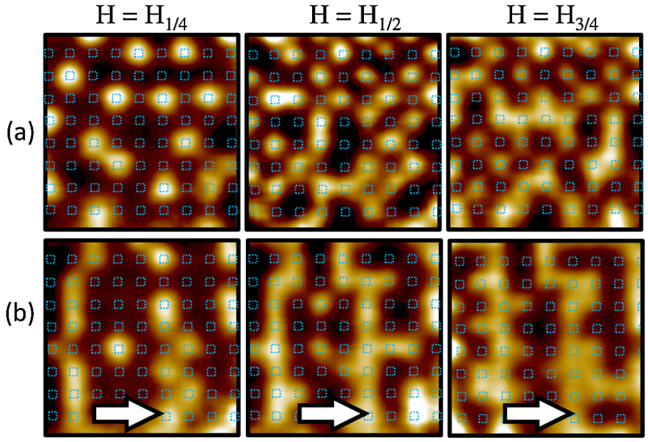

FIG. 4 (color online). Vortex configurations, imaged by SHPM at $T = 4.2$ K: (a) field cooled without applied current and (b) field cooled with applied current of 36 mA. The arrows indicate the direction of the applied current.

27 mA produces a field of 0.03 mT. This is far smaller than the field range covered in this Letter thus indicating that self-field effects are not relevant.

To summarize, we provide unambiguous evidence for the formation of kinematic vortices in a type-II superconducting film patterned with an array of antidots. These kinematic vortices attract each other forming stripe patterns that can be stabilized by literally freezing their motion via a fast thermal quench. Contrary to other systems exhibiting stripe phases [5–7], vortices in our samples have

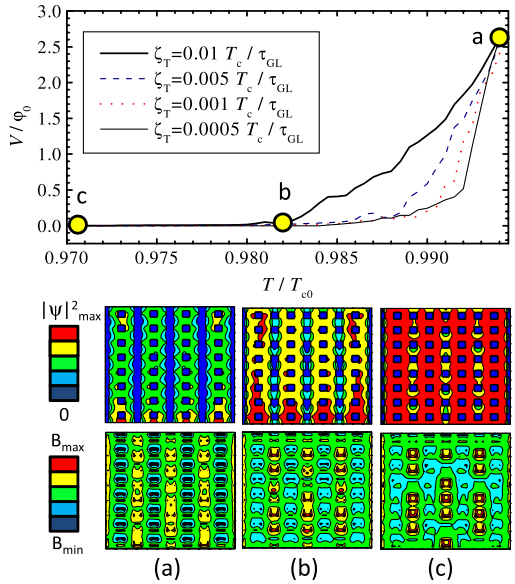

FIG. 5 (color online). Calculated voltage drop as a function of temperature, for four different cooling rates ζ_T. Panels (a)–(c) show the Cooper-pair density (top panel) and magnetic field profiles in the sample (bottom panel), for the fastest cooling case at three different T as indicated in the main panel.

no attractive interaction in equilibrium conditions, and stripe formation results solely from the dynamic history of the superconducting condensate.

This work was supported by Methusalem funding by the Flemish government, the Flemish Science Foundation (FWO-Vl), the Belgian Science Policy, and the ESF NES network. A. V. S., G. R. B., and J. V. d. V. acknowledge support from FWO-Vl. R. F. L. acknowledges support from I3P CSIC program and MAT2008-01022.

[1] C. Harisson *et al.*, Science **290**, 1558 (2000).
[2] M. Tinkham, *Introduction to Superconductivity* (McGraw-Hill, New York, 1975).
[3] T. Matsuda *et al.*, Science **294**, 2136 (2001).
[4] V. G. Kogan *et al.*, Phys. Rev. B **42**, 2631 (1990).
[5] A. I. Buzdin and A. Yu. Simonov, JETP Lett. **51**, 191 (1990); A. I. Buzdin *et al.*, Phys. Rev. B **79**, 094510 (2009).
[6] A. E. Jacobs, Phys. Rev. B **4**, 3029 (1971); J. Auer and H. Ullmaier, Phys. Rev. B **7**, 136 (1973); K. Dichtel, Phys. Lett. **35A**, 285 (1971); E. H. Brandt, Phys. Lett. **39A**, 193 (1972).
[7] V. V. Moshchalkov *et al.*, Phys. Rev. Lett. **102**, 117001 (2009).
[8] E. Babaev and M. Speight, Phys. Rev. B **72**, 180502(R) (2005).
[9] G. Malescio and G. Pellicane, Nature Mater. **2**, 97 (2003).
[10] A. I. Larkin and Yu. N. Ovchinnikov, Zh. Eksp. Teor. Fiz. **68**, 1915 (1975) [Sov. Phys. JETP **41**, 960 (1976)]; A. Andronov *et al.*, Physica (Amsterdam) **213C**, 193 (1993).
[11] D. Y. Vodolazov and F. M. Peeters, Phys. Rev. B **76**, 014521 (2007).
[12] C. J. Olson-Reichhardt *et al.*, Phys. Rev. Lett. **92**, 016801 (2004).
[13] C. Reichhardt *et al.*, Phys. Rev. Lett. **90**, 026401 (2003).
[14] A. G. Sivakov *et al.*, Phys. Rev. Lett. **91**, 267001 (2003).
[15] S. J. Bending, Adv. Phys. **48**, 449 (1999).
[16] L. Kramer and R. J. Watts-Tobin, Phys. Rev. Lett. **40**, 1041 (1978).
[17] A. N. Grigorenko *et al.*, Phys. Rev. B **63**, 052504 (2001).
[18] S. B. Field *et al.*, Phys. Rev. Lett. **88**, 067003 (2002).
[19] A. N. Grigorenko *et al.*, Phys. Rev. Lett. **90**, 237001 (2003).
[20] K. Harada, O. Kamimura, H. Kasai, T. Matsuda, A. Tonomura, and V. V. Moshchalkov, Science **274**, 1167 (1996).
[21] This time was estimated by the minimal separation time between consecutive pulses needed to obtain cumulative heating in the sample.
[22] M. Baert, V. V. Metlushko, R. Jonckheere, V. V. Moshchalkov, and Y. Bruynseraede, Phys. Rev. Lett. **74**, 3269 (1995).
[23] See supplementary material at http://link.aps.org/supplemental/10.1103/PhysRevLett.104.017001 for SHPM images obtained in a plain Pb film at 4.2 K after field cooling with and without applied current and for two different magnetic fields.